

## Experimental determination of the $^{41}\text{Ca}(n,\alpha)^{38}\text{Ar}$ reaction cross section as a function of the neutron energy

---

Liesbeth De Smet<sup>\*a</sup>, C. Wagemans<sup>a</sup>, J. Heyse<sup>b</sup>, S. Vermote<sup>a</sup> and J. Van Gils<sup>c</sup>

<sup>a</sup>University of Gent, Dept. of Subatomic and Radiation Physics,

Proeftuinstraat 86, B-9000 Gent, Belgium

<sup>b</sup>IRMM-EC-JRC, Neutron Physics Unit, Retieseweg 111, B-2440 Geel, Belgium

<sup>c</sup>SCK•CEN, Boeretang 200, B-2400 Mol, Belgium

E-mail: liesbeth.desmet@gmail.com, cyrillus.wagemans@UGent.be

The  $^{41}\text{Ca}(n,\alpha)^{38}\text{Ar}$  reaction cross section has been studied with resonance neutrons at the linear accelerator GELINA of the IRMM in Geel (Belgium) and has been determined up to 45 keV using the time-of-flight technique. A dozen resonances have been identified and for most of them the area, the total width, and a value for  $\Gamma_n/\Gamma_p$  could be determined. From the obtained cross section data the Maxwellian averaged cross section (MACS) has been calculated by numerical integration.

*International Symposium on Nuclear Astrophysics - Nuclei in the Cosmos - IX*  
25-30 June 2006  
CERN

---

\*Speaker.

## 1. Introduction

In 1978 already Woosley *et al.* [1] predicted that the  $^{41}\text{Ca}(n,\alpha)$  reaction strongly dominates over the  $^{41}\text{Ca}(n,\gamma)$  reaction at stellar temperatures of importance for s-process nucleosynthesis in stars. This has been confirmed in more recent theoretical works (S. Goriely *et al.* [2] and T. Rauscher *et al.* [3]). To verify the theoretical Maxwellian averaged (n, $\alpha$ ) cross section values (MACS), a dedicated measurement of the  $^{41}\text{Ca}(n,\alpha)^{38}\text{Ar}$  reaction cross section as a function of the neutron energy has been performed.

## 2. Experimental setup

The  $^{41}\text{Ca}(n,\alpha)^{38}\text{Ar}$  reaction was studied at the GELINA neutron time-of-flight facility of the IRMM. Two different measurement campaigns were performed to define the reaction cross section. One at an 8.5 m long flight path and a second one at 30 m to extend the energy range. For the measurement at 8.5 m, a Frisch gridded ionization chamber with methane as detector gas was used, while a 100  $\mu\text{m}$  thick surface barrier detector was used at the 30 m long flight path. For the moment, a new measurement at 30 m is ongoing, this time using an ionization chamber. Therefore, the results from the 30 m measurement are only preliminary and the results presented in this contribution are based on the measurement at 8.5 m.

For neutron induced charged particle reactions on  $^{41}\text{Ca}$ , both, (n,p) and (n, $\alpha$ ) reactions are possible. However, the settings of the ionization chamber were adjusted to detect only  $\alpha_0$ - and  $\alpha_1$ -particles. For all the measurements, the accelerator was operated at a repetition frequency of 800 Hz and the electron bursts had a width of 1 ns. To remove neutrons from previous bursts, a cadmium overlap filter at 8.5 m and a boron overlap filter at 30 m were permanently used. The time dependent background was determined in a separate measurement by putting black resonance filters such as Au, Co, Mn, Rd and W in the neutron beam.

The  $^{41}\text{Ca}$  sample used for the measurements was prepared at the IRMM by suspension spraying of  $\text{CaF}_2$  in methanol on an aluminium foil. This resulted in a  $^{41}\text{CaF}_2$  sample with 81.69% enrichment [4] containing  $(3.36 \pm 0.44) \times 10^{17}$   $^{41}\text{Ca}$  atoms on a  $6 \times 5 \text{ cm}^2$  effective area. For the neutron flux determination  $^{10}\text{B}$  layers containing  $(7.17 \pm 0.13) \times 10^{19}$  atoms were used.

The total observed counting rate  $Y_{Ca}(E_n)$  for a neutron induced reaction as a function of the neutron energy is:

$$Y_{Ca}(E_n) = \varepsilon_{Ca} N_{Ca} \sigma_{Ca}(E_n) \varphi(E_n) + Y_{Ca}^{BG}(E_n), \quad (2.1)$$

where  $\varepsilon_{Ca}$  is the detector efficiency and  $N_{Ca}$  the number of atoms in the  $^{41}\text{Ca}$  sample used.  $\sigma_{Ca}(E_n)$  is the differential neutron induced cross section to be determined and  $\varphi(E_n)$  represents the neutron flux. The time dependent background  $Y_{Ca}^{BG}$  has been determined as a function of the time-of-flight  $t$  by fitting a function  $Y_{Ca}^{BG}(t) = at^b + c$  through the counting rates in the black resonance regions and has been subtracted from the counting rate  $Y_{Ca}(t)$ . An identical relation for the flux counting rate, in our case the  $^{10}\text{B}(n,\alpha)$ -counting rate, is adopted and dividing them gives:

$$\sigma_{Ca}(E_n) = \frac{\varepsilon_B}{\varepsilon_{Ca}} \frac{Y_{Ca}(E_n) - Y_{Ca}^{BG}(E_n)}{Y_B(E_n) - Y_B^{BG}(E_n)} \frac{N_B}{N_{Ca}} \sigma_B(E_n). \quad (2.2)$$

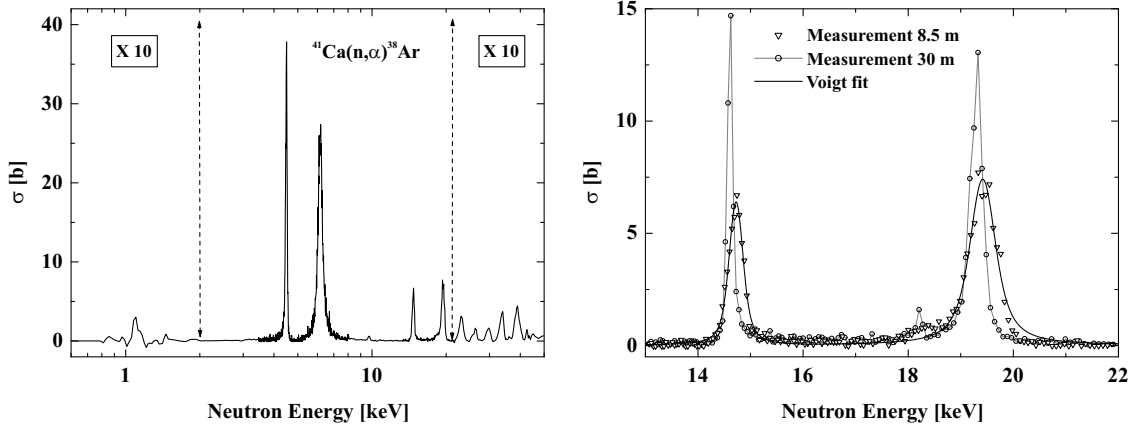


**Figure 1:** Left: The  $^{41}\text{Ca}(n,\alpha)^{38}\text{Ar}$  cross section measured at 8.5 m. Right: Voigt fits to the measured  $^{41}\text{Ca}(n,\alpha)$  cross section data for some resonances (measurement at 8.5 m). The cross section data measured at 30 m are preliminary.

For the measurements with the ionization chamber as well as with the surface barrier detector the  $^{41}\text{Ca}(n,\alpha)$  reaction and the  $^{10}\text{B}(n,\alpha)$  reaction have been measured in the same experimental conditions, so  $\frac{\epsilon_B}{\epsilon_{Ca}} = 1$  (detection geometry equals  $2\pi$ ). The known  $^{10}\text{B}(n,\alpha)$  reference cross section  $\sigma_B(E_n)$  is taken from the ENDF/B-VI database.

### 3. Results and resonance analysis

#### 3.1 Fitting procedure

Figure 1 shows the  $^{41}\text{Ca}(n,\alpha)^{38}\text{Ar}$  cross section in the neutron energy region from 600 eV to 50 keV. The resonances are fitted with Voigt shapes to determine the energy position, the area and the total level width. Such a Voigt function is a convolution of a Breit-Wigner function and a Gauss function. The Gauss shape represents the experimental broadening, which can be calculated and is taken fixed during the fit. The results of these Voigt fits are listed in the left part of table 1.  $\omega_\alpha$  is the resonance strength and is proportional to the area. The resulting Voigt fits are shown in figure 1 for the resonances at 14.73 keV and 19.43 keV. The preliminary data from the 30 m measurement are plotted with dots in figure 1. It is clear that the resolution is much better, confirming the existence of a resonance at 18.45 keV. Clearly, this better resolution will lead to a more precise determination of the level widths.

#### 3.2 Spin assignment

s-wave ( $\ell = 0$ ) neutrons impinging on  $^{41}\text{Ca}$ , ground state  $I^\pi = \frac{7}{2}^-$ , will populate the  $J^\pi = 3^-$  and  $J^\pi = 4^-$  states of the compound nucleus  $^{42}\text{Ca}$ , whereas p-wave ( $\ell = 1$ ) neutrons can populate states from  $J^\pi = 2^+$  through  $J^\pi = 5^+$ . The formed states decay to the ground ( $J^\pi = 0^+$ ) or first excited state ( $J^\pi = 2^+$ ) of  $^{38}\text{Ar}$  by emitting  $\alpha_0$ - or  $\alpha_1$ -particles, respectively. The smallest allowed angular momenta of the emitted  $\alpha$ -particles are tabulated in table 2.

| Energy [eV]                  | $\Gamma$ [eV]   | Area [b.eV]     | $\omega_\alpha$ [eV] | $\omega_p$ [eV] [7] | $\frac{\Gamma_n}{\Gamma_p}$ |
|------------------------------|-----------------|-----------------|----------------------|---------------------|-----------------------------|
| 1090 $\pm$ 70                |                 | 30 $\pm$ 15     |                      |                     |                             |
| 4490 $\pm$ 10                | 40 $\pm$ 20     | 3400 $\pm$ 300  | 3.73 $\pm$ 0.33      | 7.4                 | 8.07 $\pm$ 0.71             |
| 6170 $\pm$ 60                | 260 $\pm$ 26    | 11350 $\pm$ 950 |                      |                     |                             |
| 9725 $\pm$ 75                | 125 $\pm$ 100   | 170 $\pm$ 60    | 0.40 $\pm$ 0.14      | 9.2                 | 0.70 $\pm$ 0.25             |
| 14725 $\pm$ 75               | 175 $\pm$ 140   | 2500 $\pm$ 300  | 9.00 $\pm$ 1.08      | 2.1                 | 68.57 $\pm$ 8.24            |
| 18450 $\pm$ 300 <sup>a</sup> |                 |                 |                      |                     |                             |
| 19430 $\pm$ 150              | 420 $\pm$ 100   | 5800 $\pm$ 600  | 27.55 $\pm$ 2.86     | 1.6                 | 275.5 $\pm$ 28.6            |
| 23080 $\pm$ 200              | 600 $\pm$ 200   | 400 $\pm$ 150   | 2.26 $\pm$ 0.85      | 2.8                 | 12.90 $\pm$ 4.84            |
| 26100 $\pm$ 800 <sup>b</sup> |                 |                 |                      |                     |                             |
| 29700 $\pm$ 700              | 1250 $\pm$ 1000 | 250 $\pm$ 100   | 1.82 $\pm$ 0.73      | 2.4                 | 12.10 $\pm$ 4.85            |
| 33700 $\pm$ 700              | 1000 $\pm$ 600  | 550 $\pm$ 220   | 4.53 $\pm$ 1.82      | 5.7                 | 12.72 $\pm$ 5.09            |
| 38850 $\pm$ 1200             | 2000 $\pm$ 1200 | 900 $\pm$ 300   | 8.55 $\pm$ 2.86      | 2.9                 | 47.16 $\pm$ 15.79           |

<sup>a</sup> The resonance at 19.43 keV is a double resonance with a first level at 18.45 keV.

<sup>b</sup> Too low counting statistics, so the area has not been fitted.

**Table 1:** Left part: Resonance parameters obtained from the Voigt fits.

Right part:  $\frac{\Gamma_n}{\Gamma_p}$  for the resonances observed in this work which correspond to resonances observed by Meijer and Van Gasteren [7].

Wagemans *et al.* [5] measured the  $^{41}\text{Ca}(n_{th},\alpha_i)$  reaction cross section with thermal neutrons at the ILL in Grenoble. This thermal cross section is the sum of the tails of all s-wave resonances. From the fitted total natural line width and from the fitted area, the contribution from each resonance to the thermal cross section can be calculated. If this calculated value is higher than the measured thermal cross section, the resonance is taken as a p-wave. On the basis of these calculations it is concluded that only the resonances around 1.1 keV and 10 keV may be s-wave. Although the natural line width could not be determined for the resonance at 1.1 keV, it can be deduced from the resonance area that its thermal contribution in case of an s-wave will not exceed the measured thermal cross section. The pulse height spectra (anode and cathode) for the resonance at 1.1 keV reveal that this is a transition only to the first excited state of  $^{38}\text{Ar}$ . Taking into account the spin assignments for s-wave neutrons, the only possibility is that this resonance corresponds to a  $4^-$  state of  $^{42}\text{Ca}$ . On the contrary, the 10 keV resonance consists of  $(n,\alpha_0)$  as well as  $(n,\alpha_1)$  transitions. With the help of table 2, it is concluded that the 10 keV resonance is a  $3^-$  state in  $^{42}\text{Ca}$ . All the other resonances are considered to be p-wave. Because  $(n,\alpha_0)$  and  $(n,\alpha_1)$  transitions are observed in all of them, these resonances are most probably  $2^+$  states as  $3^+$  and  $5^+$  states are ruled out by parity constraints and the  $4^+$  state is less probable because the higher orbital momentum of the  $\alpha$ -particle reduces the penetrability through the centrifugal barrier.

In principle, interference effects between two neighbouring resonances with the same spin can reduce the contribution to the thermal cross section, leaving open the possibility of a different spin assignment for some resonances. This would lead to a non  $1/v$ -behaviour of the cross section at low neutron energy. The experimental cross section obtained in this work shows some possible

| $J^\pi \text{ } ^{38}\text{Ar}$ | $J^\pi \text{ } ^{42}\text{Ca}$ compound nucleus |       |        |       |       |       |
|---------------------------------|--|-------|--------|-------|-------|-------|
|                                 | s-wave   |       | p-wave |       |       |       |
|                                 | $3^-$  | $4^-$ | $2^+$  | $3^+$ | $4^+$ | $5^+$ |
| $0^+ (\alpha_0)$                | 3  | p.f.  | 2      | p.f.  | 4     | p.f.  |
| $2^+ (\alpha_1)$                | 1  | 3     | 0      | 2     | 2     | 4     |

p.f. = parity forbidden

**Table 2:** Smallest allowed angular momenta of the emitted  $\alpha$ -particles from the formed compound nucleus  $^{42}\text{Ca}$  in the case of impinging s- or p-wave neutrons.

interference effects between the resonances at 4.5 keV and 6.2 keV and between 14.7 keV and the doublet around 19 keV [6].

### 3.3 Determination of the partial level widths

The only additional information on  $^{42}\text{Ca}$  compound levels in the covered energy range was obtained in a proton induced reaction on  $^{41}\text{K}$  by Meijer and Van Gasteren [7]. They reported a list of  $\omega_p = (2J+1)\Gamma_p\Gamma_{\alpha_0}/\Gamma$  values for the measured  $^{41}\text{K}(p,\alpha_0)^{38}\text{Ar}$  reaction. The  $\Gamma_p$ -value from their work corresponds with  $p_0$ -decay in the case of neutron induced reactions on  $^{41}\text{Ca}$ . In the case of a neutron induced reaction on  $^{41}\text{Ca}$  only  $p_0$ - and  $p_1$ -decay to  $^{41}\text{K}$  is possible, so  $\Gamma_p = \Gamma_{p_0} + \Gamma_{p_1}$ . However, the probability that the  $p_1$ -particles penetrate the Coulomb barrier is very low since their energy is only 0.21 MeV. Therefore, it can be assumed that  $\Gamma_p = \Gamma_{p_0}$  in a neutron induced measurement. Consequently, the  $\Gamma_p$  from the measurement of Meijer and Van Gasteren [7] is equal to the  $\Gamma_p$  from this work. By dividing the fitted resonance strength  $\omega_\alpha$  obtained in this work ( $\omega_\alpha = g \frac{\Gamma_n\Gamma_\alpha}{\Gamma} = \frac{(2J+1)}{16} \frac{\Gamma_n\Gamma_\alpha}{\Gamma}$  and is proportional to the resonance area), by the reported  $\omega_p$ -value of Meijer and Van Gasteren, a value for  $\frac{\Gamma_n}{\Gamma_p}$  is obtained. The values for  $\frac{\Gamma_n}{\Gamma_p}$  for the resonances observed in this work which correspond to resonances observed by Meijer and Van Gasteren [7] are listed in table 1.

The partial widths may be calculated through combining the expressions for  $\omega_p$  and  $\omega_\alpha$  mentioned above, and the expression for the total width  $\Gamma = \Gamma_n + \Gamma_\gamma + \Gamma_p + \Gamma_\alpha$ . Five parameters ( $J$ ,  $\Gamma_n$ ,  $\Gamma_\gamma$ ,  $\Gamma_p$  and  $\Gamma_\alpha$ ) have to be fixed with only three equations at our disposal. This means that it is not possible to solve this system of equations unambiguously. For this reason no partial level widths could be determined. Additional measurements leading to the same compound nucleus  $^{42}\text{Ca}$  are necessary to determine the partial widths.

## 4. Astrophysical implications

The  $^{41}\text{Ca}(n,\alpha)$  MACS values are obtained by numerical integration of the determined cross section and are shown in figure 2. In this work the cross section is obtained up to an energy of approximately 45 keV and because a resonance at an energy  $E_{res}$  has its maximum contribution at  $kT = 0.5 E_{res}$ , the obtained MACS values above 22 keV are lower limits. In figure 2 a comparison is made with the values obtained from the MOST [2] and the NON-SMOKER [3] codes. In the energy region covered by the experiment, two stellar temperatures are of interest in s-process network

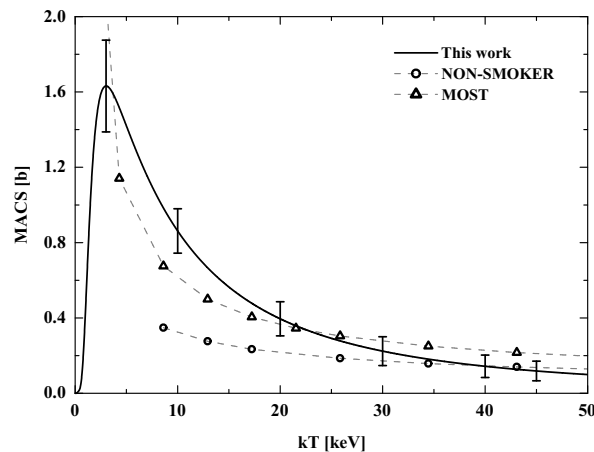


**Figure 2:** The  $^{41}\text{Ca}(n,\alpha_0+\alpha_1)^{38}\text{Ar}$  MACS values obtained by numerical integration of the obtained cross section data. A comparison is made with theoretical values.

calculations: 8 keV and 25 keV. For 8 keV, it is clear from figure 2 that both theoretical models underestimate the MACS value obtained in this work. At 25 keV, the MOST value is in agreement with the measured MACS value, but still, the NON-SMOKER value is significantly lower.

The implementation of these much higher experimental MACS values in nucleosynthesis network calculations will among others affect the  $^{36}\text{S}$  abundance.  $^{36}\text{S}$  is believed to be synthesized mainly during the weak s-process in massive stars, in particular during the convective He-core burning (at 8 keV and 25 keV) followed by convective C-shell burning (at 86 keV). To check this hypothesis, nucleosynthesis network calculations in the mass region between  $28 \leq A \leq 42$  are necessary. The  $^{41}\text{Ca}(n,\alpha)$  reaction plays a role in this network as it recycles to  $^{36}\text{S}$  via the following reaction chain:  $^{41}\text{Ca}(n,\alpha)^{38}\text{Ar}(n,\gamma)^{39}\text{Ar}(n,\alpha)^{36}\text{S}$ . Although the  $^{39}\text{Ar}(n,\alpha)^{36}\text{S}$  channel is less important than the  $^{36}\text{Cl}(n,p)^{36}\text{S}$  channel for the production of  $^{36}\text{S}$ , it is included in the stellar models. As a second part of the weak s-process occurs at temperatures around 86 keV, the additional measurement on a 30 m flight path at the GELINA facility will provide the complete MACS information needed to check the hypothesis.

## References

- [1] S. Woosley *et al.*, *At. Data and Nucl. Data Tables* **22** (1978) 371.
- [2] S. Goriely *et al.*, <http://www-astro.ulb.ac.be/Html/ncap.html>.
- [3] T. Rauscher *et al.*, <http://quasar.physik.unibas.ch/~tommy/reactlib.html>.
- [4] C. Wagemans, *Nucl. Instr. & Meth. in Physics Research* **A282** (1989) 4.
- [5] C. Wagemans, R. Bieber, H. Weigmann and P. Geltenbort, *Phys. Rev.* **C57** (1998) 1766.
- [6] M. Moxon, private communication.
- [7] R. J. Meijer and J. J. M. Van Gasteren, *Nucl. Phys.* **A148** (1970) 62.